

Altered Forebrain and Hindbrain Development in Mice Mutant for the *Gsh-2* Homeobox Gene

John C. Szucsik,* Dave P. Witte,† Hung Li,* Sarah K. Pixley,‡
Kersten M. Small,§ and S. Steven Potter*¹

*Divisions of Developmental Biology and †Division of Pathology, Children's Hospital Medical Center, Cincinnati, Ohio 45229-3039; ‡Department of Cell Biology, Neurobiology, and Anatomy, University of Cincinnati College of Medicine, Cincinnati, Ohio 45267; and §Rollins Research Center, Emory University School of Medicine, Atlanta, Georgia 30322

The patterning of the mammalian brain is orchestrated by a large battery of regulatory genes. Here we examine the developmental function of the *Gsh-2* nonclustered homeobox gene. Whole-mount and serial section *in situ* hybridizations have been used to better define *Gsh-2* expression domains within the developing forebrain, midbrain, and hindbrain. *Gsh-2* transcripts are shown to be particularly abundant in the hindbrain and within the developing ganglionic eminences of the forebrain. In addition, mice carrying a targeted mutation of *Gsh-2* have been generated and characterized. Homozygous mutants uniformly failed to survive more than 1 day following birth. At the physiologic level the mutants experienced apnea and reduced levels of hemoglobin oxygenation. Histologically, the mutant brains had striking alterations of discrete components. In the forebrain the lateral ganglionic eminence was reduced in size. In the hindbrain, the area postrema, an important cardiorespiratory chemosensory center, was absent. The contiguous nucleus tractus solitarius, involved in integrating sensory input to maintain homeostasis, was also severely malformed in mutants. Immunohistochemistry was used to examine the mutant brains for alterations in the distribution of markers specific for serotonergic and cholinergic neurons. In addition, *in situ* hybridizations were used to define expression patterns of the *Dlx 2* and *Nkx 2.1* homeobox genes in *Gsh-2* mutant mice. The mutant lateral ganglionic eminences showed an abnormal absence of *Dlx 2* expression. These results better define the genetic program of development of the mammalian brain, support neuromeric models of brain development, and further suggest similar patterning function for homeobox genes in phylogenetically diverse organisms. © 1997 Academic Press

Key Words: homeobox gene; brain development; gene targeting.

INTRODUCTION

The development of the brain is a complex multistep process. The folding of the neural plate forms the neural tube. The undifferentiated neuroepithelium of the rostral neural tube then bulges, flexes, and constricts to form the prosencephalon, mesencephalon, and rhombencephalon, which give rise to the forebrain, midbrain, and hindbrain, respectively. The adult mammalian brain is an extremely elaborate structure. The human brain, for example, consists of thousands of types of neurons and about 10^{11} total neurons associated with more than 10^{12} glial cells (Kandel *et*

al., 1991). Adding to the complexity, the average cortical neuron correctly synapses with 10,000 others. Understanding the genetic basis of brain development presents a major challenge.

Homeobox genes often occupy high-level positions in the genetic hierarchy of development. This evolutionarily conserved family of genes encodes transcription factors with a 60-amino acid helix–turn–helix motif, the homeodomain (reviewed by Gehring, 1987). These genes are broadly divided into two groups. In mammals, the 39 genes that reside within the four main clusters are designated Hox genes, while the remaining chromosomally scattered or orphan genes, of even greater but still uncertain number, are usually named after their *Drosophila* homologues. The clustered Hox genes show a striking colinearity between their position within the cluster and their expression domain in the developing embryo (Graham *et al.*, 1989). Genes more 3' in the clusters are expressed earlier and in more rostral

¹ To whom correspondence should be addressed at Division of Developmental Biology, Children's Hospital Research Foundation, 3333 Burnet Avenue, Cincinnati, OH 45229-3039. Fax: 513-636-4317. E-mail: steve.potter@chmcc.org.

domains. In contrast, the nonclustered homeobox genes have diverse expression patterns (Kern *et al.*, 1992; Li *et al.*, 1994; Valerius *et al.*, 1995). Mutations in the *Drosophila* clustered homeobox genes often result in homeotic transformations of segment identity or structure deletions (McGinnis and Krumlauf, 1992).

Abundant evidence indicates that homeobox genes play critical roles in brain development. The Hox genes show overlapping domains of expression in the rhombomeres of the developing hindbrain (Keynes and Krumlauf, 1994). Ectopic expression of Hox genes, induced by retinoic acid or heterologous promoters, can generate partial transformations of rhombomere identity (Marshall *et al.*, 1992; Zhang *et al.*, 1994). Likewise, targeted mutations of Hox genes can influence hindbrain development. In *Hoxa 1* mutants, for example, there is a deletion of rhombomere 5 as well as a dramatic reduction in the size of rhombomere 4 (Lufkin *et al.*, 1991; Chisaka *et al.*, 1992; Dolle *et al.*, 1993; Carpenter *et al.*, 1993). Nevertheless, the clustered Hox genes are not expressed rostral to rhombomere 2 of the hindbrain (Keynes and Krumlauf, 1994). This indicates that other genes are responsible for pattern formation in these regions. Indeed, more than 25 nonclustered homeobox genes, including the vertebrate homologs of the *Drosophila* *Engrailed*, *Distal-less*, and *empty spiracles* genes, are expressed in the developing midbrain and forebrain (reviewed by Rubenstein and Puelles, 1994).

We have previously described the isolation of a pair of murine homeobox genes, designated *Gsh-1* and *Gsh-2*, with no known *Drosophila* homologues (Singh *et al.*, 1991). These two genes are closely related, encoding homeodomains that are identical at 58 of 60 amino acid positions. *Gsh-1* and *Gsh-2* map chromosomally to two distinct positions on chromosome five and are not associated with the four main clusters of Hox genes. Nevertheless, these genes are very Hox-like in two respects. Among all nonclustered homeobox genes their encoded homeodomains are most closely related to those encoded by the Hox genes. Indeed, their encoded homeodomains are more "Antennapedia-like" than those of many Hox genes (Singh *et al.*, 1991). Furthermore, their genomic organization, with but a single small intron, closely resembles that seen for many Hox genes and is distinct from that found for most nonclustered homeobox genes.

Gsh-1 and *Gsh-2* appear to function in the formation of the brain. They are transcribed in partially overlapping domains in the developing brain. *Gsh-1* and *Gsh-2* are expressed in the developing ganglionic eminences and diencephalon of the forebrain and in restricted regions of the developing mid- and hindbrain (Valerius *et al.*, 1995; Hsieh-Li *et al.*, 1995). Moreover, we have previously reported the targeted deletion of *Gsh-1* (Li *et al.*, 1996). The resulting homozygous mutants have hypothalamic defects, with the arcuate nucleus no longer synthesizing growth hormone-releasing hormone. This creates a severe dwarfism, caused by a hypocellular pituitary with a greatly reduced population of growth hormone-producing somatotrophs.

In this report we describe the targeted mutation of the

Gsh-2 homeobox gene. The resulting homozygous mutant mice, which die within the first day following birth, are shown to have interesting brain malformations. In the hindbrain, the area postrema and nucleus tractus solitarius, important for cardiorespiratory control, suffer major structural deletions. In the forebrain the lateral ganglionic eminence is reduced in size and perturbed in its gene expression pattern.

MATERIALS AND METHODS

Construction of the *Gsh-2* Targeting Vector

An isogenic replacement targeting vector was generated using a 129/SVJ mouse genomic DNA library (provided by Tom Doetschman). A multipurpose knockout vector, pMCKOV, previously described (Li *et al.*, 1994) was used as the backbone to make the pMCKO *Gsh-2* construct. A 9-kb *Xba*I fragment was used as the long block of homology while the short block of homology consisted of a 0.8-kb *Not*I/*Eco*RI fragment. Plasmid DNA was prepared by cesium chloride banding, linearized, and used for electroporation as previously described (Li *et al.*, 1994).

Generation of *Gsh-2* Targeted Mice

D3 ES cells maintained on mitomycin C-treated G418^r mouse embryo fibroblast feeder cells were electroporated with the pMCKO *Gsh-2* vector. Positive and negative selection, using G418 and ganciclovir, respectively, were as previously described (Li *et al.*, 1994). A total of 320 individual colonies were picked and screened for homologous recombination. DNAs were pooled into groups of six and initially screened by PCR using nested primers from the 3' end of the neo cassette and the 5' end of the DNA flanking the short block of homology. The outer oligos were 5'-CAGGACATAGCGTTGGCTACCCGTGATATT-3' and 5'-CGC-TCTACCTTTGCTCAAAGCCAGTTCTC-3', and the inner oligos were 5'-CATCGCCTTCTATCGCCTTCTTGACGAGTT-3' and 5'-CACCCACCACAGCATCATCACCATCAC-3', for *neo* and *Gsh-2*, respectively. It was necessary to include 5% formamide in the PCR cocktail to amplify this GC-rich region of DNA. Once correctly targeted pools of DNA were identified, PCR and Southern blot analysis were used to identify and confirm individual targeted clones. A 1-kb *Not*I-*Hind*III fragment was used as a flanking probe on Southern blot analysis and gave diagnostic bands of 9.3, 3.5, and 3.6 kb for *Hind*III, *Hind*III, and *Eco*RV and *Bst*II restriction endonuclease digestions, respectively (data not shown).

C57Bl/6J blastocysts (day 3.5 p.c.) were isolated from uteri of superovulated mice, injected with targeted ES cells, and transferred to pseudopregnant mice as previously described (Li *et al.*, 1994).

Histological Analysis

Embryos or neonate heads were fixed overnight in Bouin's solution followed by extensive rinsing and dehydration in 70% ethanol. Samples were then fully dehydrated in ascending ethanol baths, cleared in xylene, and embedded in paraffin. Serial sections were cut on a microtome at 15 μ m thickness and Nissl stains performed. Lungs were dissected out of neonates and fixed overnight with 4% paraformaldehyde/PBS at 4°C. The following day, samples were rinsed in 70% ethanol and processed as above.

Immunohistochemistry

Neonate brains were dissected from the cranium and fixed overnight in 4% paraformaldehyde/PBS at 4°C. Following fixation the brains were rinsed and dehydrated with 70% ethanol. Samples were further dehydrated in ascending alcohol baths, cleared in xylene, and paraffin embedded. Serial sections were cut on a microtome at 15 μ m thickness and collected on glass slides. Just prior to use, sections were deparaffinized in xylene and rehydrated in descending ethanol baths. Primary antisera consisted of anti-choline acetyltransferase (Chemicon) and anti-tryptophan hydroxylase (Chemicon) used at a 1:100 dilution and incubated at 4°C overnight. An avidin/biotin immunoperoxidase system (ABC system/Vector) was used to detect antibody binding according to supplied protocols.

Blood Gas Measurements

Blood gas measurements were performed on neonates using a Corning 170 pH/blood gas analyzer. Animals were decapitated and blood samples immediately collected in heparinized microhematocrit capillary tubes and analyzed. Readings were collected and a one-way ANOVA statistical analysis was performed. Noninvasive measurements of blood oxygenation levels were also determined with a laser oxymeter generously provided by Dr. Michael Donnelly.

In Situ Hybridizations

Serial section and whole-mount *in situ* hybridizations were performed as previously described (Li et al., 1994). The *Gsh-2* probe used was also previously described (Hsieh-Li et al., 1995).

RESULTS

Gsh-2 Developmental Expression

The *Gsh-2* gene is expressed in discrete domains during early brain development. We previously described the distribution of *Gsh-2* transcripts in embryos using serial section *in situ* hybridization (Hsieh-Li et al., 1995). Signal was detected in the ganglionic eminences and diencephalon of the forebrain, as well as restricted regions of the mid- and hindbrain. In this report we extend the expression analysis to include whole-mount *in situ* hybridizations at earlier time points as well as serial section *in situ* hybridizations that include later time points than previously examined.

Gsh-2 expression was first detected in E9 embryos where it localized to regions of the primitive neuroepithelial layer in the telencephalic vesicle, neuroepithelium of the third ventricle adjacent to the hypothalamic sulcus, and to bands extending from the neural tube rostrally into the developing hindbrain (Fig. 1A). These studies revealed a dynamic, developmentally regulated spatial and temporal expression pattern. At E9 the hindbrain expression was strictly caudal of the otic vesicles, but by E10 the expression extended well rostral of the otic vesicles (Fig. 1B). Transverse sections showed that the expression of *Gsh-2* at E10 was within the alar plate of the developing neural tube (Fig. 1C). At E12 the embryos showed a persistent strong hybridization signal

in the ganglionic eminences and around the third ventricle in the developing thalamic nuclei, as well as a band of signal that extended ventrally toward the floor of the third ventricle (Hsieh-Li et al., 1995). At E14 *Gsh-2* transcripts were localized in the medial ganglionic eminences (MGE) and in the lateral ganglionic eminences (LGE) (Fig. 1D). At this time point (E14) no hybridization signal was detected in the developing spinal cord or around the fourth ventricle. By the newborn stage (Fig. 1E) the hybridization signal was weak and essentially restricted to a small cluster of cells overlying the basal ganglia in the subependymal region of the lateral ventricles.

Targeted Disruption of the *Gsh-2* Gene

To better define its developmental function *Gsh-2* was disrupted by homologous recombination in embryonic stem cells. The replacement construct, illustrated in Fig. 2A, was designed to inactivate *Gsh-2* by deleting the region encoding the DNA recognition helix of the homeodomain. Homologous recombination between the pMCKO *Gsh-2* targeting construct and the *Gsh-2* gene resulted in a deletion of 487 bp. This removed coding sequences for the last 40 amino acids of the homeodomain and the carboxy terminus of the protein. The construct was electroporated into D3 ES cells and 320 clones were screened for homologous recombination, with a single targeted clone identified and confirmed by Southern analysis (data not shown).

Blastocyst injections and implantations into pseudopregnant mice to produce chimeras were as previously described (Li et al., 1994). The heterozygous progeny of these chimeras were indistinguishable from wild type. They were healthy and fertile and had a normal lifespan. The *Gsh-2*^{+/-} mice were mated to generate *Gsh-2*^{-/-} offspring, which were genotyped as shown in Fig. 2B.

The *Gsh-2* Mutant Phenotype

The *Gsh-2* gene is not required for survival to birth. One hundred fifty-seven newborn offspring of heterozygous matings were genotyped, giving a normal Mendelian distribution, with 36 (22.9%) wild types, 86 (54.8%) heterozygotes, and 35 (22.3%) homozygotes (mutants). There was no evidence of prenatal loss of homozygous mutants. Furthermore, at birth the homozygous mutants were of normal weight and grossly identical to heterozygous and wild-type littermates.

The *Gsh-2* gene is, however, required for continued postnatal survival. No mutant animals lived beyond 24 h after birth. The *Gsh-2*^{-/-} neonates suffered from apnea. The mutant pups exhibited periods of normal skin coloration and breathing, with lung inflation observed grossly through the chest wall, followed by episodes of cyanotic appearance and cessation of breathing. Blood gas measurements of neonates indicated that the mutants were hypoxic (Fig. 3). The blood oxygen levels (pO₂ mm Hg) of the mutant pups measured only 63.9 (\pm 7.1 SEM, *n* = 11), which was significantly lower

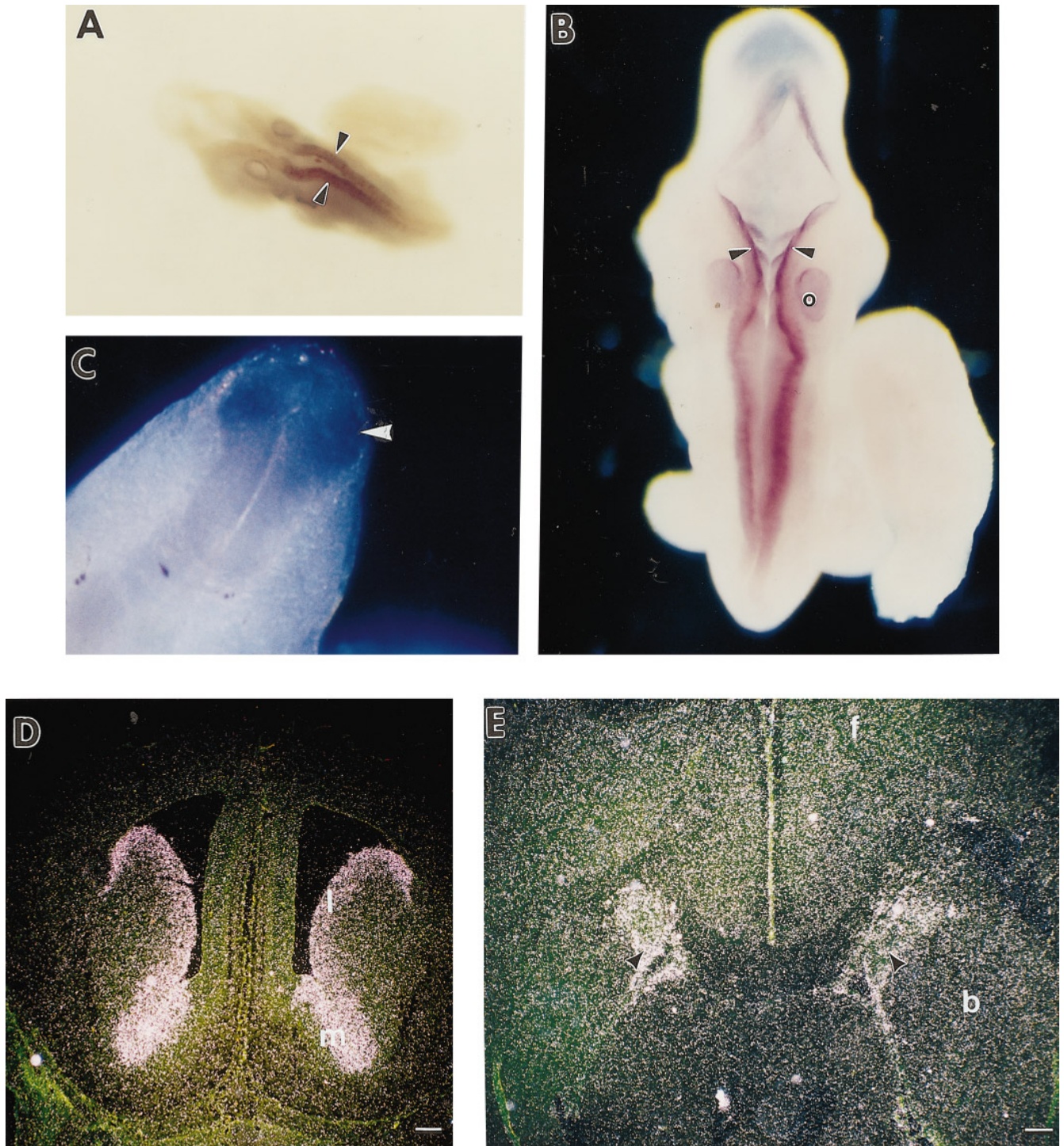
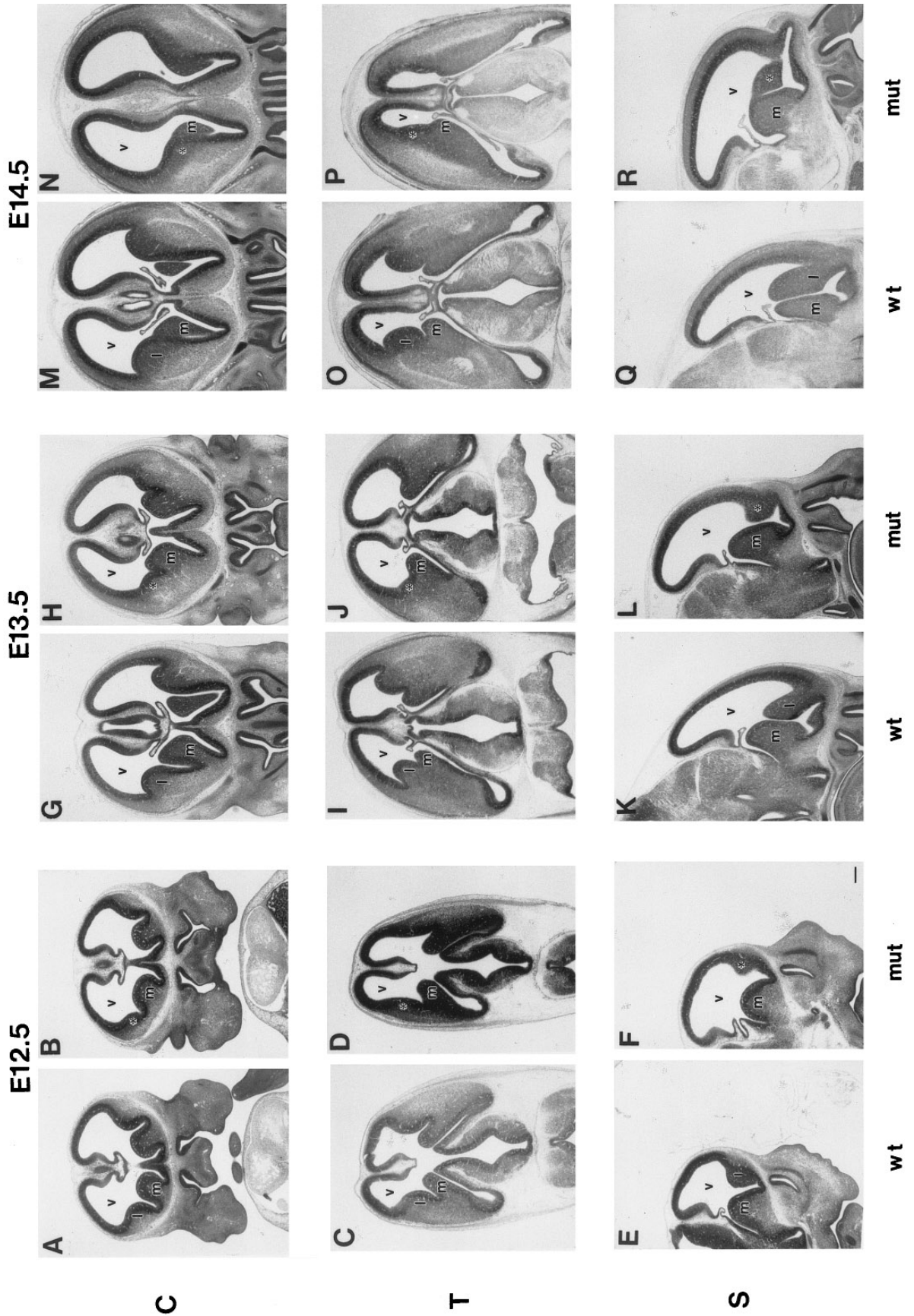


FIG. 1. Localization of *Gsh-2* transcripts during development. (A) Whole-mount *in situ* hybridization at E9 shows *Gsh-2* expression (arrowheads) in the developing neural tube below the level of the otic vesicle. (B) One day later in development, at E10, expression in the hindbrain (arrowheads) extends well rostral of the otic vesicles. Staining of the otic vesicles in A and B is also seen with the sense control probe and is therefore likely due to nonspecific trapping. (C) In a cross-section through the neural tube at E10 *Gsh-2* expression is limited to the dorsal aspect or developing alar plate region (arrowhead). (D) Serial section *in situ* hybridization indicates *Gsh-2* expression at E14 in the neuroepithelium of the MGE and LGE. (E) *Gsh-2* expression in the neonate brain (horizontal section) is weak, although clearly present in this long exposure, and restricted to cells beneath the ependymal lining and overlying the basal ganglia region of the lateral ventricles (arrowheads). b, basal ganglia; f, frontal cortex; l, lateral ganglionic eminence; m, medial ganglionic eminence; o, otic vesicle. Size bar indicates 125 μ m.



Interestingly, the *Gsh-2*^{-/-} neonates exhibiting apnea could be temporarily revived by tactile stimulation. The blood gas measurements described above were performed using a Corning 170 blood gas analyzer that requires withdrawn blood, allowing only one time point per neonate. In addition, however, a noninvasive laser oxymeter that allowed continual time course readings of blood oxygenation levels was used. It was observed that handling the mutants markedly increased the fraction of hemoglobin with bound oxygen (data not shown). The effect was temporary, however, and even prolonged handling did not extend survival beyond 24 h.

In addition, the mutants had normal hematocrits, and skeletal stains revealed no apparent structural defects (data not shown). The absence of milk spots in all mutants indicated a failure to feed, but this was not likely the cause of death, as most mutants died within hours of birth.

Central Nervous System Defects

To search for potential developmental defects, the brains of *Gsh-2* mutants, heterozygotes, and wild-type littermate controls were subjected to histological analysis. The developmental time points of E12.5, E13.5, E14.5, E15.5, E17.5, and newborn were studied. The histological analysis included sagittal, frontal, and transverse planes at each time point. Furthermore, the phenotype was characterized on both a 129/CF-1 hybrid genetic background and a 129 inbred background. The results are summarized below and were the same for both genetic backgrounds.

Discrete defects were observed in the developing basal ganglia of the homozygous mutant forebrains. In particular, there was a significant reduction in the size of the LGE. At E12.5, E13.5, and E14.5, as determined by frontal, transverse, and parasagittal sections, the LGE was reduced (Fig. 4). This decreased mass of the LGE persisted at later time points (data not shown).

Histological examination also revealed hindbrain malformations in *Gsh-2*^{-/-} mutants. This again corresponded to a region of high *Gsh-2* expression during development. The area postrema, a circumventricular organ, and the adjacent nucleus tractus solitarius (NTS), both important in the control of cardiorespiratory physiology, failed to develop properly in mutants. Parasagittal sections through wild-type (Fig.

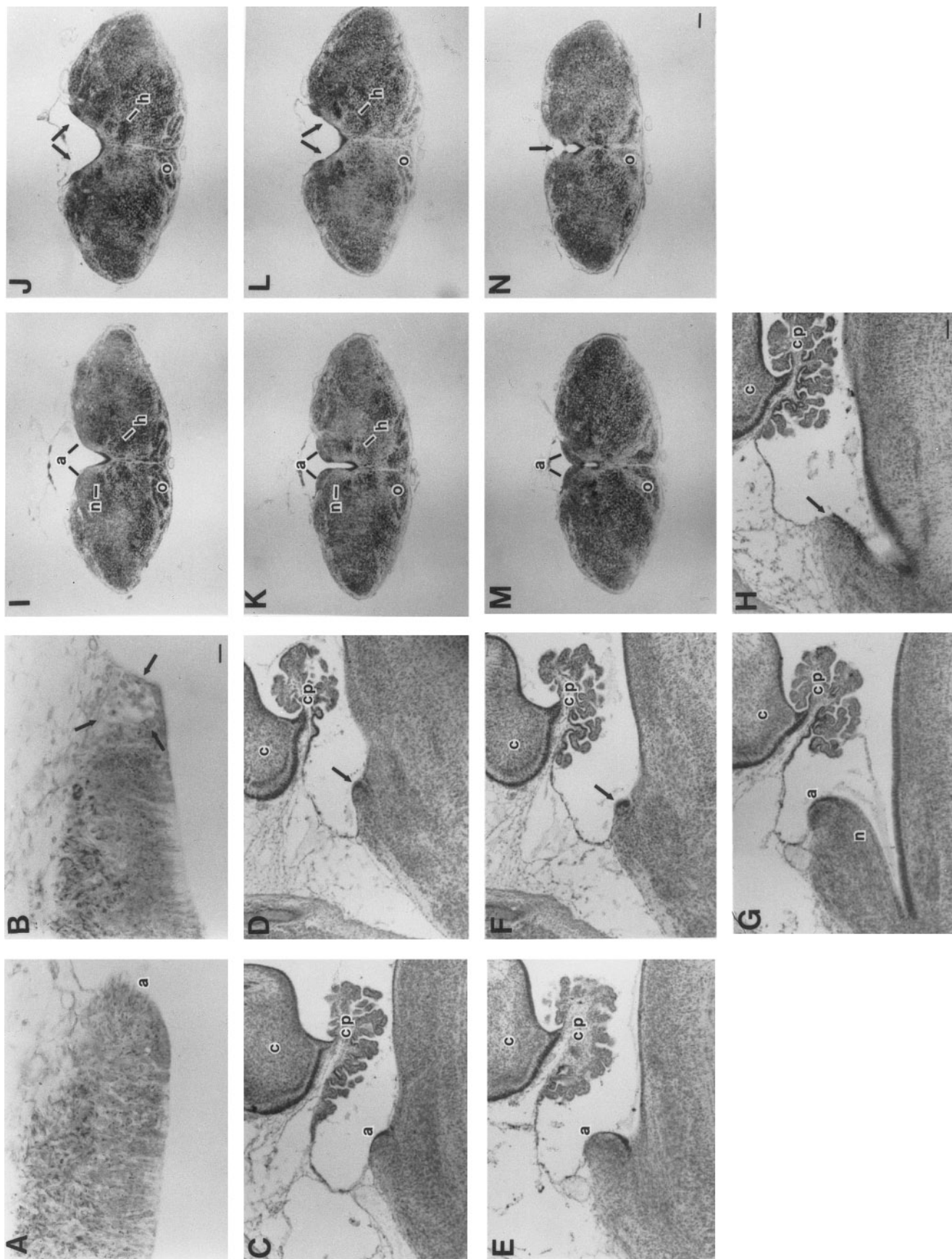
5A) and mutant (Fig. 5B) E15.5 hindbrains showed that the developing area postrema was hypocellular. Two days later in gestation, at E17.5, the differences were more pronounced. Figures 5C, 5E, and 5G show the progression from lateral to medial parasagittal hindbrain sections in a wild-type embryo and demonstrate normal area postrema and underlying NTS (Barraco et al., 1992). In corresponding mutant littermates (Figs. 5D, 5F, and 5H), however, the area postrema did not form and the underlying NTS was reduced in size. This was even more pronounced in the neonate hindbrains. Figures 5I, 5K, and 5M show frontal sections (rostral to caudal) of a wild-type newborn hindbrain. The area postrema was evident at the base of the fourth ventricle and posteriorly fused at the dorsal midline to become the dorsal tissue over the central canal of the spinal cord. In the mutant brainstem (Figs. 5J, 5L, and 5N) the area postrema failed to develop, and the larger opening of the fourth ventricle resulted from a deficit in the NTS, which normally lies immediately ventral to the area postrema and immediately lateral to the fourth ventricle. The observed malformations of the area postrema and NTS correlate with both the developmental expression pattern of *Gsh-2* in the hindbrain and the phenotype of apnea and hypoxia seen in the mutant pups. Heterozygous brains appeared normal (data not shown).

Gsh-2 is most similar to another dispersed mouse homeobox gene, *Gsh-1*, with identity at 58 of 60 amino acids in the encoded homeodomains (Singh et al., 1991). Expression of both genes is largely limited to the central nervous system, and there is partial overlap in their patterns of expression in the mesencephalon and diencephalon (Hsieh-Li et al., 1995; Valerius et al., 1995). The anterior pituitary of *Gsh-1*^{-/-} mice was found to be hypocellular and showed a decrease in the number of acidophilic somatotrophs and lactotrophs (Li et al., 1996). To determine if *Gsh-2* plays a role in pituitary development tissue sections from mutant brains were examined and stained to define acidophiles and basophiles. The anterior pituitary was normal in size and cellularity, and no abnormalities in the differentiation of cell types were detected (data not shown).

Immunohistochemistry

The histological analysis demonstrated the importance of the *Gsh-2* gene in development of the ganglionic eminences

FIG. 5. Abnormal hindbrain development in *Gsh-2*^{-/-} mice. Parasagittal sections through the developing E15.5 area postrema show normal development and cellularity in the wild-type animal (A) and hypocellularity of the area postrema in the mutant (arrows, B). (E–H) Parasagittal sections, lateral to more medial, through the hindbrain of wild-type and mutant E17.5 embryos. The wild-type embryo (C, E, and G) shows normal development of the area postrema and the underlying nucleus tractus solitarius. In the mutant embryo (D, F, and H), however, the area postrema fails to form (arrows) and the underlying nucleus tractus solitarius is reduced in size. (I–N) Neonate frontal sections showing progression from rostral to caudal hindbrain. The wild-type hindbrain (I, K, and M) shows the formation of the area postrema and closing of the dorsal region of the medulla to form the central canal of the spinal cord. The *Gsh-2*^{-/-} hindbrain (J, L, and N) does not form an area postrema and the dorsal medial medulla corresponding to the nucleus tractus solitarius region is also affected as seen by the wider fourth ventricle opening (arrows). The fourth ventricle does close in more caudal sections, leaving a larger opening of the central canal. a, area postrema; c, cerebellum; cp, choroid plexus; h, hypoglossal nucleus; n, nucleus tractus solitarius; o, inferior olive. Size bar indicates 25 μm in B, 125 μm in H, and 200 μm in N.



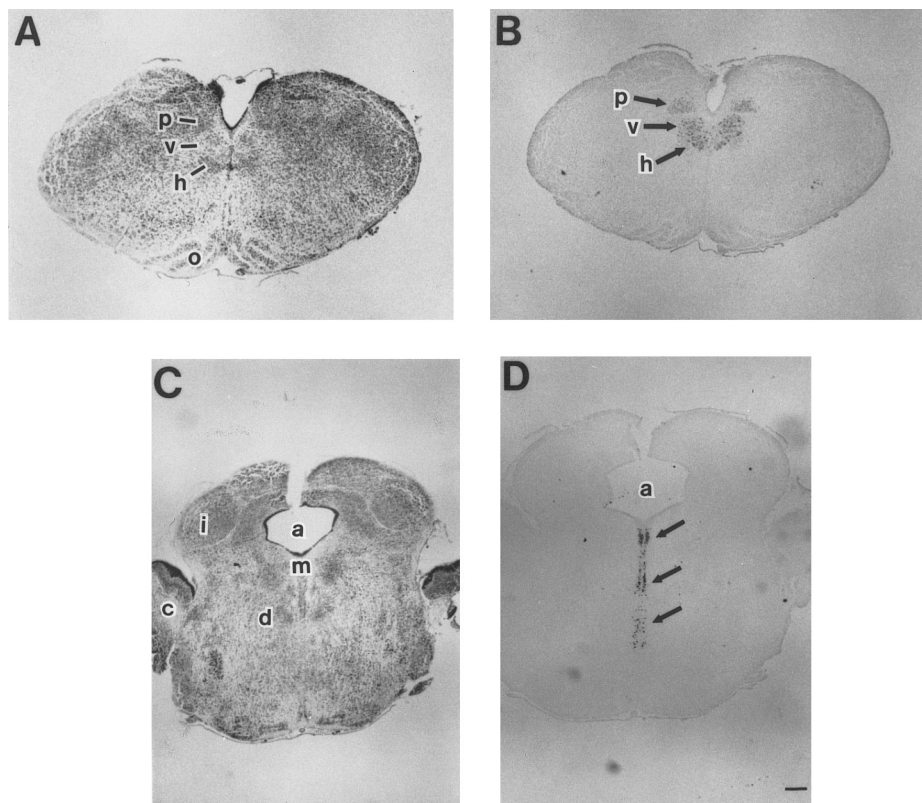


FIG. 6. Immunohistochemical analysis of *Gsh-2*^{-/-} brains. Nissl stained section through the medulla of a mutant brain (A). An adjacent serial section (B) was reacted with an antibody specific for choline acetyltransferase and shows labeling of neurons in the dorsal motor nucleus of the vagus, as well as the hypoglossal and prepositus nuclei. Nissl stained section through the pons of a mutant brain (C). Serial section (D) reacted with an antibody specific for tryptophan hydroxylase, with intense labeling of neurons in the medial longitudinal fasciculus (arrow). No differences were seen in comparing wild-type and mutant brains. a, Aqueduct of Sylvius; c, cerebellum; d, dorsal tegmental nucleus; h, hypoglossal nucleus; i, inferior colliculus; m, medial longitudinal fasciculus; p, prepositus nucleus, v, dorsal motor of vagus nucleus. Size bar indicates 125 μ m.

of the forebrain as well as the area postrema and NTS of the hindbrain. Nevertheless, other regions of *Gsh-2* expression, including the diencephalon, appeared histologically normal. This could be the result of an absence of *Gsh-2* developmental function in these areas or the result of functional redundancy with the closely related *Gsh-1* gene. Alternatively, subtle defects may be present that were not detectable histologically. To begin to address this issue immunohistochemistry was used to assay the expression patterns of neuronal markers. Entire brains from *Gsh-2*^{-/-} and *Gsh-2*^{+/+} animals were serially sectioned and reacted with anti-tryptophan hydroxylase and anti-choline acetyltransferase antibodies to compare the distributions of serotonergic and cholinergic neurons, respectively. These markers have expression domains that include and flank regions of *Gsh-2* expression and provide a molecular assay for developmental perturbation that might not be detected by histology.

Acetylcholine transferase expression was observed in discrete patterns in the thalamus and hypothalamus and more caudally in the pons. The highest levels were seen in the hindbrain in the prepositus, dorsal motor of the vagus, and hypoglossal nuclei (Figs. 6A and 6B). Three mutant and

wild-type neonates were compared. No differences in the distributions of cholinergic neurons were found between wild-type and mutant brains.

The most rostral expression of tryptophan hydroxylase was seen at low but detectable levels starting in the caudate-putamen region in neonates. More caudal sections showed stronger levels of expression scattered throughout the thalamus and hypothalamus, with localized expression seen in the subthalamic nucleus. The highest tryptophan hydroxylase levels were seen in the pons in the ventral tegmentum and the isthmus of the cerebellum (Figs. 6C and 6D). Again, three wild-type brains and three mutant brains were serially sectioned and compared. No differences in the distribution patterns of serotonergic neurons were detected. In addition, cranial nerve distribution was examined using an anti-neurofilament antibody. Again, no additional differences between wild-type and mutant were observed (data not shown).

Expression Patterns of the *Nkx 2.1* and *Dlx 2* Homeobox Genes in *Gsh-2* Mutant Mice

The possible molecular level perturbation of development in *Gsh-2* mutants was further pursued by *in situ* hybridiza-

tion analysis of the expression patterns of three homeobox genes normally transcribed in the developing forebrain. Two of these genes, *Nkx 2.1* and *Nkx 2.2*, belong to the NK gene family originally discovered in *Drosophila* (Kim and Nirenberg, 1989). *Nkx 2.1* and *Nkx 2.2* have patterns of expression that overlap with each other and with that of *Gsh-2* (Lazzaro *et al.*, 1991; Price *et al.*, 1992; Price, 1993; Rubenstein and Puelles, 1994). Of particular interest here, *Nkx 2.1* is normally expressed in the developing MGE. In comparing E12 wild-type and homozygous *Gsh-2* mutants no difference in *Nkx 2.1* expression was observed (Figs. 7A and 7B).

We also examined ganglionic eminence development in mutant mice by *in situ* hybridization using a *Dlx 2* probe. The mouse *Dlx 1* and *Dlx 2* genes are homologs of the *Drosophila* distal-less homeobox gene. The normal expression patterns of the *Dlx 1* and *Dlx 2* genes have been described, with both genes expressed in a similar fashion in both the MGE and the LGE during development (Price *et al.*, 1991; Porteus *et al.*, 1991; Robinson *et al.*, 1991; Dolle *et al.*, 1992; Price, 1993). *In situ* hybridizations with the *Dlx 2* probe revealed a dramatic difference in expression between wild-type and *Gsh-2* mutant E12 embryos (Figs. 7C and 7D). Once again, both the wild-type and mutant MGE showed expression. However, while the wild-type LGE expressed abundant *Dlx 2* transcripts, the mutant LGE showed no detectable hybridization signal. Therefore, the mutant LGE is not only reduced in size, but also shows an abnormal gene expression pattern. Of interest, in the mutant MGE there is also apparently reduced expression of *Dlx 2* in the neuroepithelium immediately flanking the ventricles (Figs. 7E and 7F), suggesting the presence of subtle MGE abnormalities.

DISCUSSION

In this report we extend the previous *Gsh-2* expression studies and describe the *Gsh-2* mutant phenotype. Expression of *Gsh-2* in the hindbrain was observed to be dynamic, with transcripts detected in the neural tube and most caudal region of the developing hindbrain at E9. One day later the boundary of *Gsh-2* expression in the hindbrain extended to include regions rostral to the otic vesicles. *Gsh-2* expression in the hindbrain then faded, with no hybridization signal detected at E14.5. *Gsh-2* transcription was also seen in parts of the diencephalon and in the ganglionic eminences of the developing forebrain. Expression in the forebrain also decreased with time, being barely detectable in newborns.

Targeted mutation of the *Gsh-2* gene resulted in alterations of discrete structures of the brain, representing a subset of *Gsh-2* expression domains. In the developing forebrain histologic sections showed a reduction in size of the LGE, which gives rise to the striatum in the adult brain. The basal ganglia consist of multiple subcortical nuclei, including the globus pallidus, the subthalamic nucleus, the substantia nigra, the putamen, and caudate nucleus. The putamen and caudate nucleus comprise the striatum. Diseases of the basal ganglia generally result in involuntary movement dis-

orders that include tremors, chorea, and ballism (violent, flailing movements).

The targeted mutation of *Gsh-2* also severely perturbs development of the area postrema and subpostremal region of the NTS in the hindbrain. Indeed, in homozygous mutants only remnants of these structures appear to remain. The observed disruption of hindbrain development in *Gsh-2* mutants indicates that the nonclustered homeobox genes, as well as the previously studied Hox genes, play an important role in the morphogenesis of the hindbrain. The hindbrains of the *Gsh-2* animals show malformations which are coincident with high levels of *Gsh-2* expression during development of the dorsal-medial medulla. These malformations are in turn consistent with the mutant phenotype of apnea and hypoxia since this region of the brainstem is an important cardiorespiratory regulator.

The area postrema is a chemosensory center at the blood-brain interface of the fourth ventricle (Ferguson, 1991). It is an important target for information reaching the brainstem through the blood supply for the maintenance of homeostasis (Johnson and Gross, 1993). Surgical ablation of the area postrema in rats results in hypotension and marked bradycardia (Skoog and Mangiapane, 1988).

The NTS is a Y-shaped tract of neuronal cell bodies located in the dorsal-medial medulla adjacent to the fourth ventricle and area postrema (Barraco *et al.*, 1992). It functions as the major integrative visceral sensory nucleus of the brainstem through the afferent connections it receives from mechano-, baro-, and chemoreceptors, while also serving a major visceral efferent function through its connections with regulatory regions within the ventral-lateral medulla. The subpostremal region of the NTS, deleted in *Gsh-2* mutants, serves as the major integrator of cardiopulmonary afferent information to control cardiorespiratory homeostasis. It also has extensive connections with virtually all rostral brain sites involved in cardiorespiratory control, homeostatic maintenance, and metabolic regulation. It is therefore not surprising that disruption of this region of the brainstem is fatal in the *Gsh-2*^{-/-} animals at the critical transition from uterine to external life. Motor function in the *Gsh-2* mutants appears intact as assayed by the ability of these animals to inflate their lungs and breath for periods of time. Morphologically and biochemically the mutant lungs appear normal. Nevertheless, the newborns exhibit periods of apnea, at the physiologic level they are hypoxic, and at the histological level they show an absence of specific hindbrain structures derived from the alar plate. These observations are all consistent with a critical deficit in the sensory components of the cardiorespiratory control center of the hindbrain.

Several models have been proposed to account for the regionalization of the forebrain during development. Columnar model(s) have been described by His (1893), Herrick (1910), and Kuhlenbeck (1973). Neuromeric models have more recently been proposed. Figdor and Stern (1993) used injections of tracer dyes in developing forebrain cells to define neuromere boundaries that block cell mixing. In addition, morphological structures and expression patterns of

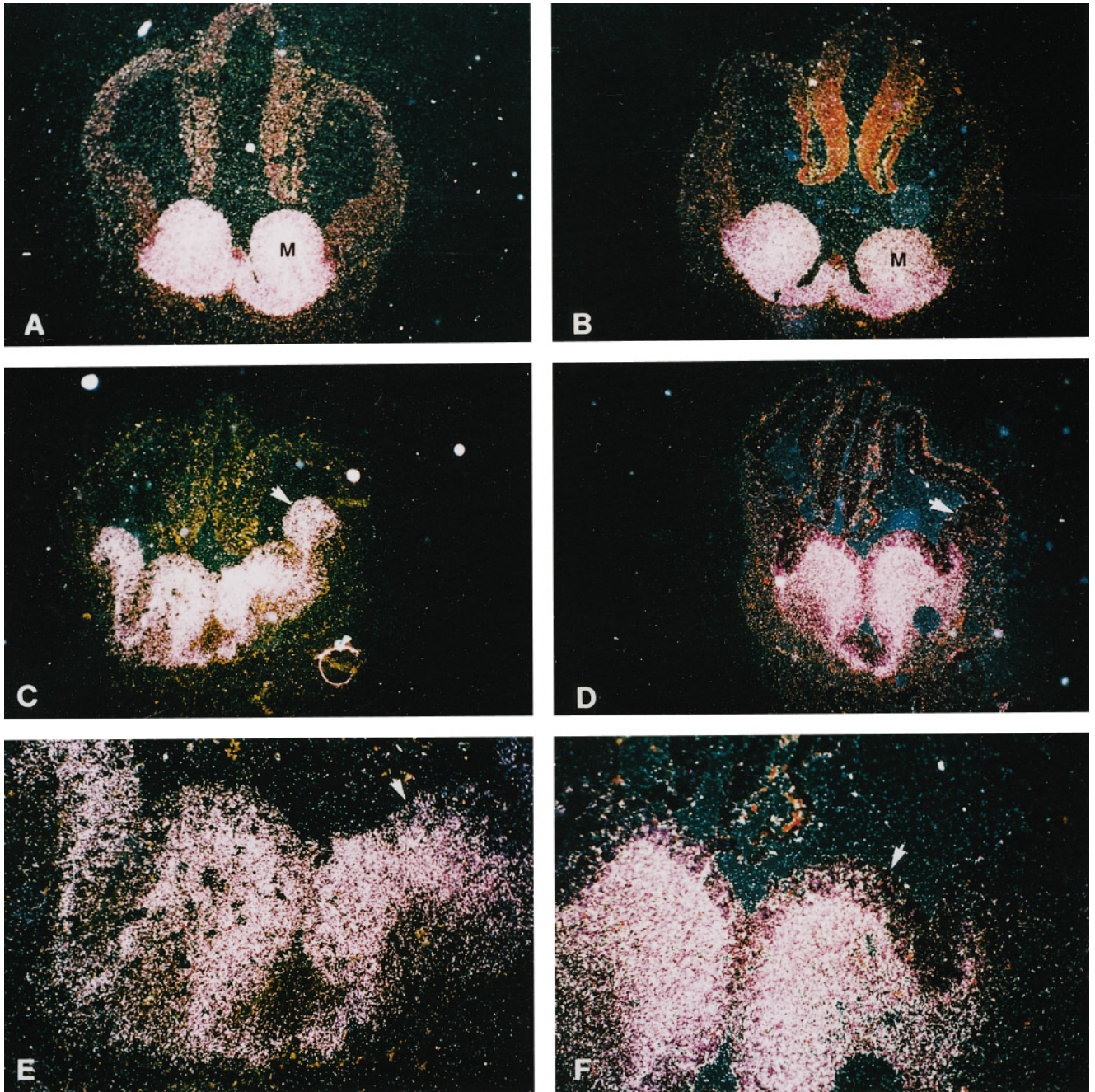


FIG. 7. Expression patterns of *Nkx 2.1* and *Dlx 2* in *Gsh-2* mutant mice. A–G are dark-field photomicrographs of coronal sections through the brains of E12 embryos. Wild-type mice are shown in A, C, and E. *Gsh-2* homozygote mutants are shown in B, D, F, and G. The expression pattern of *Nkx 2.1* is restricted to the MGE (M) in both wild-type (A) and mutant (B). In contrast, *Dlx 2* is expressed in the wild-type embryo (C) in both the MGE and LGE (arrowhead), while the *Gsh-2* mutant (D) shows expression in the MGE but not in the LGE (arrowhead). E is a higher magnification of C, and F is a higher magnification of D. These panels show less expression of *Dlx 2* in a band of neuroepithelial cells (arrowhead) overlying the MGE in the *Gsh-2* mutant (F) in contrast to the more intense uniform signal in the same region (arrowhead) of the wild-type embryo (E).

cell adhesion molecules, acetylcholinesterase, and a battery of regulatory genes were used to divide the diencephalon into four neuromeres. Puellas and Rubenstein (1993) have also described a neuromeric model, with boundaries of neu-

romeres based primarily on an extensive analysis of expression domains of regulatory genes. The alterations of discrete brain structures in the *Gsh-2* mutants further demonstrate the importance of such regulatory genes in brain develop-

ment and suggest that the use of their expression domains in constructing neuromere boundaries represents a valid approach.

The deletion of discrete components of the hindbrain and alterations in gene expression programs in the forebrains of *Gsh-2* mutants further support the view that homeobox genes fulfill similar developmental roles in *Drosophila* and mammals. Mutations of Hom-C (clustered homeobox) genes in *Drosophila* often result in either homeotic transformations of segment identity or structure deletions (McGinnis and Krumlauf, 1992). The ectopic expression of *Antennapedia* resulting in the conversion of the developmental program of an imaginal disc to generate a leg in place of an antennae is indeed remarkable (Gibson *et al.*, 1990). It is perhaps equally informative, however, that mutations of the *labial*, *proboscopedia*, and *Deformed* homeobox genes result in deletions of structures (Merrill *et al.*, 1987, 1989; Pultz *et al.*, 1988). If a gene is responsible for initiating a genetic cascade that results in the formation of a particular structure, then when the gene is inactivated the structure will not form. Alternatively, if other key Hox genes remain expressed, then the Hox code (Lewis, 1978) and resulting structure identity are changed.

The functional characterization described in this report places *Gsh-2* among a growing list of genes now shown to be important in brain development. In mice mutant for the *En-1* gene, another dispersed homeobox gene, extensive regions of the mid- and hindbrain are absent (Wurst *et al.*, 1994). This phenotype is similar to that of *Wnt1* mutants (McMahon and Bradley, 1990), which is not surprising since the *Drosophila* homologues of *Wnt-1* and *En-1* are known to interact (DiNardo *et al.*, 1988). Mutations of *Gsh-1* and *Gsh-4* cause hypothalamic and hindbrain defects, respectively (Li *et al.*, 1994, 1996). Of particular interest, mutations in the *Otx2* and *Lim1* dispersed homeobox genes result in massive deletions of rostral head structures. The *Otx2* mutation removes all structures rostral to rhombomere 3 (Matsuo *et al.*, 1995), and the *Lim1* mutation similarly results in essentially "headless" mice (Shawlot and Behringer, 1995). It is noteworthy that mutations in most of the genes mentioned above result in related phenotypes, with deletions of CNS structures. Earlier acting genes, such as *Otx2* and *Lim1*, have broader effects than later acting genes such as *Gsh-1* and *Gsh-2*, suggesting that they initiate genetic programs which eventually result in the start of subprograms. If a key gene in the genetic hierarchy of a program or subprogram is absent, then the program does not properly execute and the structure does not form.

As the coarse roles of homeobox genes expressed in the developing brain are determined by mutational analysis, the field moves toward a better understanding of brain development. Many genes remain to be examined and individual mice mutant for multiple genes will need to be made to address functional redundancy. At the molecular level, however, the homeobox genes function by regulating expression levels of other genes. To achieve a deeper understanding of the genetic programs of brain development it

will be necessary to identify and characterize these gene targets.

ACKNOWLEDGMENTS

We thank Kathy Saalfeld and Pamela Groen for technical assistance with the serial section *in situ* hybridizations, William Bradford for help with whole-mount *in situ* hybridizations, William Pickens for help with statistical analysis of data, Ken Kramer and Richard Drake for performing glycogen assays, Michael Donnelly for use of the laser oxymeter, Susan Wert for histological examination of lung tissues, John Rubenstein and Melanie Price for *Dlx-2* and *Nkx-1-2* probe constructs, and Janice Hagedorn for expert secretarial assistance. This work was supported by National Institutes of Health Grants HD29599 (S.S.P.) and ES07051 (J.C.S.).

REFERENCES

- Barraco, R., El-Ridi, M., Ergene, E., Parizon, M., and Bradley, D. (1992). An atlas of the rat subpostremal nucleus tractus solitarius. *Brain Res. Bull.* **29**, 703–765.
- Carpenter, E. M., Goddard, J. M., Chisaka, O., Manley, N. R., and Capecchi, M. R. (1993). Loss of Hox-A1 function results in the reorganization of the murine hindbrain. *Development* **118**, 1063–1075.
- Chisaka, O., Musci, T. S., and Capecchi, M. R. (1992). Developmental defects of the ear, cranial nerves and hindbrain resulting from targeted disruption of the mouse homeobox gene Hox-1.6. *Nature* **355**, 516–620.
- DiNardo, S., Shen, E., Heemskerk-Jongens, J., Kassis, J. A., and O'Farrel, P. H. (1988). Two-tiered regulation of spatially patterned engrailed gene expression during *Drosophila* embryogenesis. *Nature* **332**, 604–609.
- Dolle, P., Price, M., and Duboule, D. (1992). Expression of the murine *Dlx-1* homeobox gene during facial, ocular and limb development. *Differentiation* **49**, 93–99.
- Dolle, P., Lufkin, T., Krumlauf, R., Mark, M., Duboule, D., and Chambon, P. (1993). Local alterations of Krox-20 and Hox gene expression in the hindbrain suggest lack of rhombomeres 4 and 5 in Hoxa 1 mutant embryos. *Proc. Natl. Acad. Sci. USA* **90**, 7666–7670.
- Ferguson, A. (1991). The area postrema: A cardiovascular control center at the blood-brain interface. *Can. J. Physiol. Pharmacol.* **69**, 1026–1034.
- Figdor, M. C., and Stern, C. D. (1993). Segmental organization of embryonic diencephalon. *Nature* **363**, 630–634.
- Gehring, W. J. (1987). Homeo boxes in the study of development. *Science* **236**, 1245–1252.
- Gibson, G., Schier, A., LeMotte, P., and Gehring, W. J. (1990). The specificities of *Sex combs reduced* and *Antennapedia* are defined by a distinct portion of each protein that includes the homeodomain. *Cell* **62**, 1087–1103.
- Graham, A., Papalopulu, N., and Krumlauf, R. (1989). The murine and *Drosophila* homeobox gene complexes have common features of organization and expression. *Cell* **57**, 367–378.
- Herrick, C. J. (1910). The morphology of the forebrain in amphibia and reptilia. *J. Comp. Neurol.* **20**, 413–547.
- His, W. (1893). Über die frontale ende des gehirurohes. *Arch. Anat. Entwicklungsgesch (Leipzig)*, 157–171.
- Hsieh-Li, H. M., Witte, D. W., Szucsik, J. C., Weinstein, M., Li, H.,

- and Potter, S. S. (1995). *Gsh-2*, a murine homeobox gene expressed in the developing brain. *Mech. Dev.* **50**, 177–186.
- Johnson, A. K., and Gross, P. M. (1993). Sensory circumventricular organs and brain homeostatic pathways. *FASEB J.* **7**, 678–686.
- Kandel, E. R., Schwartz, J. H., and Jessel, T. M. (1991). "Principles of Neural Science." Appleton and Lange, Norwalk, CT.
- Kern, M. J., Witte, D. P., Valerius, M. T., Aronow, B. J., and Potter, S. S. (1992). A novel murine homeobox gene isolated by a tissue specific PCR cloning strategy. *Nucleic Acids Res.* **20**, 5189–5195.
- Keynes, R., and Krumlauf, R. (1994). Hox genes and regionalization of the nervous system. *Annu. Rev. Neurosci.* **17**, 109–132.
- Kim, Y., and Nirenberg, M. (1989). *Drosophila* NK-homeobox genes. *Proc. Natl. Acad. Sci. USA* **86**, 7716–7720.
- Kuhlenbeck, H. (1973). "The Central Nervous System of Vertebrates." Karger, Basel.
- Lazzaro, D., Price, M., De Felice, M., and Di Lauro, R. (1991). The transcription factor TTF-1 is expressed at the onset of thyroid and lung morphogenesis in restricted regions of the foetal brain. *Development* **113**, 1093–1104.
- Lewis, E. B. (1978). A gene complex controlling segmentation in *Drosophila*. *Nature* **276**, 565–570.
- Li, H., Witte, D. P., Branford, W. W., Aronow, B. J., Weinstein, M., Kaur, S., Wert, S., Singh, G., Schreiner, C. M., Whitsett, J. A., Scott, W. J., and Potter, S. S. (1994). *Gsh-4* encodes a LIM-type homeodomain, is expressed in the developing central nervous system and is required for early postnatal survival. *EMBO J.* **13**, 2876–2885.
- Li, H., Zeitler, P. S., Valerius, M. T., Small, K., and Potter, S. S. (1996). *Gsh-1*, an orphan Hox gene, is required for normal pituitary development. *EMBO J.* **15**, 714–724.
- Lufkin, T., Dierich, A., LeMeur, M., Mark, M., and Chambon, P. (1991). Disruption of the Hox-1.6 homeobox gene results in defects in a region corresponding to its rostral domain of expression. *Cell* **66**, 1105–1119.
- Marshall, H., Nonchev, S., Sham, M. H., Muchamore, I., Lumsden, A., and Krumlauf, R. (1992). Retinoic acid alters hindbrain Hox code and induces transformation of rhombomeres 2/3 into a 4/5 identity. *Nature* **360**, 737–741.
- Matsuo, I., Kuratani, S., Kimura, C., Takeda, N., and Shimichi, A. (1995). Mouse Otx2 functions in the formation and patterning of the rostral head. *Genes Dev.* **9**, 2646–2658.
- McGinnis, W., and Krumlauf, R. (1992). Homeobox genes and axial patterning. *Cell* **68**, 283–302.
- McMahon, A. P., and Bradley, A. (1990). The Wnt-1 (int-1) proto-oncogene is required for development of a large region of the mouse brain. *Cell* **69**, 581–595.
- Merrill, V. K. L., Turner, F. R., and Kaufman, T. C. (1987). A genetic and developmental analysis of mutations in the *Deformed* locus in *Drosophila melanogaster*. *Dev. Biol.* **122**, 379–395.
- Merrill, V. K. L., Diederich, R. J., Turner, F. R., and Kaufman, T. C. (1989). A genetic and developmental analysis of mutations in *labial*, a gene necessary for proper head formation in *Drosophila melanogaster*. *Dev. Biol.* **135**, 376–391.
- Porteus, M. H., Bulfone, A., Ciaranello, R. D., and Rubenstein, J. L. R. (1991). Isolation and characterization of a novel cDNA clone encoding a homeodomain that is developmentally regulated in the ventral forebrain. *Neuron* **7**, 221–229.
- Price, M. (1993). Members of the *Dlx*- and *Nkx2*- gene families are regionally expressed in the developing forebrain. *J. Neurobiol.* **24**, 1385–1399.
- Price, M., Lazzaro, D., Pohl, T., Mattei, M.-G., Ruther, U., Olivo, J.-C., Duboule, D., and Di Lauro, R. (1992). Regional expression of the homeobox gene *Nkx-2.2* in the developing mammalian forebrain. *Neuron* **8**, 241–255.
- Price, M., Lemaistre, M., Pischetola, M., Di Lauro, R., and Duboule, D. (1991). A mouse gene related to *Distal-less* shows a restricted expression in the developing forebrain. *Nature* **351**, 748–751.
- Puelles, L., and Rubenstein, J. L. R. (1993). Expression patterns of homeobox and other putative regulatory genes in the embryonic mouse forebrain suggest a neuromeric organization. *Trends Neurol. Sci.* **16**, 472–479.
- Pultz, M. A., Diederich, R. J., Cribbs, D. L., and Kaufman, T. C. (1988). The *proboscipedia* locus of the Antennapedia complex: A molecular and genetic analysis. *Genes Dev.* **2**, 901–920.
- Robinson, G. W., Wray, S., and Mahon, K. A. (1991). Spatially restricted expression of a member of a new family of murine *Distal-less* homeobox genes in the developing forebrain. *New Biologist* **3**, 1183–1194.
- Rubenstein, J. L. R., and Puelles, L. (1994). Homeobox gene expression during development of the vertebrate brain. *Curr. Top. Dev. Biol.* **29**, 1–63.
- Shawlot, W., and Behringer, R. R. (1995). Requirement for *Lim1* in Head-organizer function. *Nature* **374**, 425–430.
- Singh, G., Kaur, S., Stock, J. L., Jenkins, N. A., Gilbert, D. J., Copeland, N. G., and Potter, S. S. (1991). Identification of 10 murine homeobox genes. *Proc. Natl. Acad. Sci. USA* **88**, 10706–10710.
- Skoog, K. M., and Mangiapane, M. L. (1988). Area postrema and cardiovascular regulation in rats. *Am. J. Physiol.* **254**, H963–H969.
- Valerius, M. T., Li, H., Stock, J., Weinstein, M., Kaur, S., Singh, G., and Potter, S. S. (1995). *Gsh-1*: A novel murine homeobox gene expressed in the central nervous system. *Dev. Dynam.* **203**, 337–351.
- Wigglesworth, J. S., Winston, R. M. L., and Bartlett, K. (1977). Influence of the central nervous system on fetal lung development. Experimental study. *Arch. Dis. Child.* **52**, 965–967.
- Wurst, W., Auerbach, A. B., and Joyner, A. L. (1994). Multiple developmental defects in *Engrailed-1* mutant mice: An early mid-hindbrain deletion and patterning defects in forelimbs and sternum. *Development* **120**, 2065–2075.
- Zhang, M., Kim, H.-J., Marshall, H., Gendron-Maguire, M., Lucas, D. A., Baron, A., Gudas, L. J., Gridley, T., Krumlauf, R., and Grippo, J. F. (1994). Ectopic *Hoxa-1* induces rhombomere transformation in mouse hindbrain. *Development* **120**, 2431–2442.

Received for publication May 9, 1997

Accepted September 4, 1997